Published in final edited form as:

Oncogene. 2020 May ; 39(22): 4358–4374. doi:10.1038/s41388-020-1281-9.

Intratumor δ-catenin heterogeneity driven by genomic rearrangement dictates growth factor dependent prostate cancer progression

Mingchuan Li[1,2,*], **Jongdee Nopparat**[1,3,*], **Byron J. Aguilar**[1], **Yan-hua Chen**[1], **Jiao Zhang**[1], **Jie Du**[4], **Xin Ai**[5], **Yong Luo**[2], **Yongguang Jiang**[2,#], **Christi Boykin**[1], **Qun Lu**[1,2,6,#]

[1]Department of Anatomy and Cell Biology, The Brody school of Medicine, East Carolina University, Greenville, North Carolina, USA 27834;

[2]Department of Urological Surgery, Beijing An Zhen Hospital, Capital Medical University, Beijing, China;

[3]Department of Anatomy, Prince of Songkla University, Songkhla, Thailand;

[4]Beijing Institute of Heart, Lung, and Blood Vessel Diseases, Beijing An Zhen Hospital, Capital Medical University, Beijing, China;

[5]Dept. of Urology, PLA Army General Hospital, Beijing, China;

[6]The Harriet and John Wooten Laboratory for Alzheimer's and Neurodegenerative Diseases Research, The Brody School of Medicine, East Carolina University, Greenville, North Carolina, USA 27834

Abstract

Only a small number of genes are *bona fide* oncogenes and tumor suppressors such as *Ras, Myc, β-catenin, p53* and *APC*. However, targeting these cancer drivers frequently fail to demonstrate sustained cancer remission. Tumor heterogeneity and evolution contribute to cancer resistance and pose challenges for cancer therapy due to differential genomic rearrangement and expression driving distinct tumor responses to treatments. Here we report that intratumor heterogeneity of Wnt/β-catenin modulator δ-catenin controls individual cell behavior to promote cancer. The differential intratumor subcellular localization of δ-catenin mirrors its compartmentalization in prostate cancer xenograft cultures as result of mutation-rendered δ-catenin truncations. Wildtype and δ-catenin mutants displayed distinct protein interactomes that highlight rewiring of signal networks. Localization specific δ-catenin mutants influenced $p120^{ctn}$-dependent Rho GTPase phosphorylation and shifted cells towards differential bFGF-responsive growth and motility, a known signal to bypass androgen receptor dependence. Mutant δ-catenin promoted Myc-induced

[#:]Corresponding authors: For Correspondence: Dr. Qun Lu, Professor of Anatomy and Cell Biology, The Brody school of Medicine, East Carolina University, Greenville, North Carolina, USA 27834, luq@ecu.edu, 252-744-2844.

[*:]First authors in alphabetic order

AUTHOR CONTRIBUTIONS

QL conceived the project. QL, YGJ, YHC, JD, and XA co-designed the collaboration and experiments. MCL, JN, JZ, BJA, CB, YHC, YGJ and QL performed experiments and data analyses. All authors contributed to the discussion section and approved the manuscript for submission.

CONFLICT OF INTEREST

All authors declare that there was no conflict of interests.

prostate tumorigenesis while increasing bFGF-p38 MAP kinase signaling, β-catenin-HIF-1α expression, and the nuclear size. Therefore, intratumor δ-catenin heterogeneity originated from genetic remodeling promotes prostate cancer expansion towards androgen independent signaling, supporting a neomorphism model paradigm for targeting tumor progression.

Keywords

Wnt/β-catenin modulator; intratumor heterogeneity; fibroblast growth factor; MAP kinase; Myc; rewiring interactomes

INTRODUCTION

The progression of carcinomas is associated with epithelial-to-mesenchyme transition (EMT) accompanied by the shift of gene expression profiles from cell-cell to cell-extracellular matrix interactions.[1,2] Dysregulation of many *bona fide* oncogenes and tumor suppressors such as Ras, Myc, β-catenin, p53, and APC ultimately drives the disruption of E-cadherin cell-cell junction, a signature of cancer invasion towards metastasis.

The stabilization of E-cadherin cell-cell junctions is controlled by interactions with its associated peripheral proteins such as β-catenin (*CTNNB1*), δ-catenin (*CTNND2*), and p120^{ctn} (*CTNND1*), the latter two of which bind to the same juxta-membrane domain on E-cadherin.[3] E-cadherin and p120^{ctn} often downregulate concurrently as tumor suppressors and contribute to tumor progression. On the other hand, δ-catenin expression in normal epithelial cells interferes with cell proliferation.[4–6] Then, in malignant cancers, δ-catenin overexpression increased cell growth.[7,8] It is not clear how δ-catenin exerts the context-dependent roles in cancer progression. However, δ-catenin is not the only protein that shows the dichotomy of both pro-oncogenic and tumor-suppressive functions.[2,9]

Our recent studies showed that δ-catenin overexpression in prostate cancer (PCa) cells induced mutagenesis of δ-catenin.[10] PCa xenograft cells harboring *δ-catenin* mutations showed prolonged survival when compared to PCa cells without δ-catenin overexpression or with full-length δ-catenin expression under glucose deprivation.[10] Furthermore, a δ-catenin truncation mutant promoted prostate tumorigenesis in mice with oncogenic *Myc* overexpression, supporting that δ-catenin mutants may become neomorphic and gain novel functions to promote tumor development.[10,11] Although we do not fully understand the molecular mechanisms of how the truncated δ-catenin promotes tumor progression, the truncation may reduce the ability of δ-catenin to inhibit small GTPase RhoA[5,12] and prevent the cytokinesis checkpoint-initiated apoptosis.

It is now well recognized that cancers are heterogeneous and are comprised of multiple subpopulations of cancer cells that differ in important properties, such as growth rate, cancer initiation, ability to metastasize, and sensitivity to treatments. Different cells within the same tumor can behave differently to coordinate cancer expansion.[13,14] However, little is known about how changes in oncoproteins regulate the distinct behaviors of individual cells in the same tumor. In this study, we investigate the origin of intratumor heterogeneity of one such oncoprotein, δ-catenin, corresponding to genetic aberrations. PCa metastasized to

lymph nodes as well as the neuroendocrine PCa in human showed prominent amplifications, fusions, and mutations in *δ-catenin* gene. Full-length and mutation-rendered δ-catenin truncation variants rewired their signaling networks. Intratumor δ-catenin heterogeneity promoted PCa cell motility and altered their MAP kinase responses to bFGF stimulation, a known androgen receptor bypass mechanism.[15] δ-Catenin mutations promoted mouse prostate tumorigenesis by modulating oncogenic Myc functions, revealing differential p44/42 ERK/p38 MAPK activation and β-catenin-HIF-1α stabilization.

RESULTS

Intratumor heterogeneity of δ-catenin expression *in vivo* mirrors its differential compartmentalization/localization/distribution in PCa xenograft cell lines overexpressing δ-catenin

We previously reported that even the expression of the same gene, such as *CTNND2*/δ-catenin, can be enriched at various subcellular locations in different regions of the same tumor.[16] To further investigate the potential functional implications of δ-catenin on intratumor heterogeneity, we determined δ-catenin localization/distribution in various regions of prostate tumor and in several PCa cell lines including CWR22Rv1 (Fig. 1) and LNCaP and PC3 (Supp. Fig 1). Consistent with our previous report, in the luminal side of prostatic tumors, E-cadherin and $p120^{ctn}$ colocalized in the intact adherens junction (Fig. 1A, E-cad and $p120^{ctn}$, arrows). Additionally, δ-catenin colocalized with E-cadherin and $p120^{ctn}$, showing a junction-associated distribution (JAD) (Fig 1A, δ-Cat, arrows). However, δ-catenin also showed a non-junctional, cytoplasm-associated distribution (CAD) away from the luminal side (Fig. 1A, δ-Cat, circles) or perinuclear localization at the tumor boundary (Fig. 1A, δ-Cat, arrowheads) where the E-cadherin adherens junction is weakened (Fig. 1A, E-cad and $p120^{ctn}$, arrowheads).

We then stably overexpressed GFP-tagged δ-catenin in CWR22Rv1 cells termed Rv1-M6 (Fig. 1B and 1C). As expected, δ-catenin (1B and 1C, green) showed different localization patterns even in the same transfected population of cell clusters. In some cells, δ-catenin displayed strong non-junctional staining of actin/cytoplasm-associated distribution (AAD/CAD, Fig. 1B and 1C, δ-catenin/green; left panels, arrowheads and outline), reminiscent of dotted/cytoplasmic localization in human prostatic tumor (Fig.1A; δ-catenin, circles). In other cells, δ-catenin showed adherens/cell-cell junction-associated distribution (JAD) in the center of Rv1-M6 cell cluster (Fig. 1B and 1C, δ-catenin/green; right panels, arrows). Thus, as more mutant/truncated δ-catenin is produced, there is a shift from JAD δ-catenin to AAD/CAD due to carboxyl terminal truncation as result of induced mutagenesis.[10] This is observed in several PCa cell lines (CWR22Rv1, LNCaP, and PC3) that have been passaged after the overexpression of δ-catenin.

For comparison, we transfected metastatic PCa cell lines (LNCaP-M6 and PC3-T4) with δ-catenin (Supp. Fig. 1). PC3 cells are derived from bone metastasis while LNCaP cells are derived from the left supraclavicular lymph node metastasis. As such, PC3 cells represent a more aggressive PCa form, sharing features with small cell neuroendocrine carcinoma.[17] LNCaP cells, on the other hand, are characteristic of adenocarcinoma, an indolent and

less severe PCa form.[17] LNCaP-M6 cells showed localization of δ-catenin, E-cadherin, and p-120^{ctn} similar to that of Rv1-M6 cells (Supp. Fig. 1A, green and red).

Our previous studies showed that δ-catenin overexpression in PC3 cells led to complete carboxyl terminal truncation as result of induced mutagenesis.[10] As such, PC3-T4 cells did not show JAD, but rather CAD δ-catenin (Supp. Fig. 1B, green). In this case, E-cadherin and p120^{ctn} expression was decreased as well as compared to that of LNCaP cells (Supp. Fig. 1B, red). LNCaP-M6 cells express several junction-related proteins such as claudin-7 and claudin-3.[18] On the other hand, PC3 cells has been reported to have downregulated junction-related genes.[19] A noticeable pattern across the two cell lines is a weaker p120^{ctn} and E-cadherin staining on PC3 cells versus LNCaP cells. Thus, differences in δ-catenin localization, even after overexpression of δ-catenin, may be associated with the different cellular profiles in LNCaP and PC3 cells.

δ-Catenin genetic alteration is exemplified in metastatic human PCa as well as neuroendocrine tumors

The changes in expression and distribution of δ-catenin in the primary prostatic tumors and the xenograft cell lines indicated that δ-catenin overexpression could lead to induced mutagenesis with subsequent impact on PCa progression.[10] If so, we may see extensive overexpression and mutations in the more advanced and metastatic human PCa. To test this hypothesis, we examined metastatic tissues, such as lymph nodes, from PCa patients.

As shown in Fig 2A, full-length δ-catenin migrated around 160 kDa on SDS gel, consistent with previous studies.[7,10,16] δ-Catenin can display various peptide species including the 100 kDa variant, which reflects the sequence insertion or deletions that resulted in truncations as shown in our earlier studies.[10] We observed a striking increase in δ-catenin truncation in most of the lymph node metastases (Fig. 2A). In control lymph nodes, there was minimal overexpression of δ-catenin and less truncations (Fig. 2A and Supp. Fig. 2).

We then applied sequencing and analyzed the entire coding region of *δ-catenin* gene (exons 1–22) isolated from human PCa lymph node metastases. As previously reported,[10] Sanger sequencing data presented extensive SNP profile in *δ-catenin* gene. Most functional mutations occurred in Exon 13, Exon 14, Exon 21, and Exon 22 (Supplemental Table I). We did not observe significant mutations at the amino terminus corresponding to exons 1–9. There were overall fewer mutations (Fig. 2B) and insertions (Fig. 2C) detected in normal control. These data suggest that human *δ-catenin* gene contains increased alterations in metastasis lymph nodes compared with normal control.

Furthermore, we have detected new features of *δ-catenin* genomic DNA that harbors many insertion fragments. After retrieval and comparison with GENEBANK, these insertion mutations were mapped and assigned to human genomic DNA, with interesting profile: most of these insertions came from genes that play important roles in apoptosis, such as Death-associated protein 1 (DAP), Cytolethal distending toxins (CDTs), and Carbonic anhydrase-related protein 10 (CA10), etc. Additional profiles include gene fusion involving androgen, cell adhesion and Wnt signaling, such as the SDK1, DKK3, and ERVK-5 genes.

The function of aggregation of gene sequences stemming from one signaling pathway to δ-catenin gene was not clear at the present.

We also examined a public database of *δ-catenin* gene alterations in neuroendocrine (NEN) PCa, since NEN PCa represents aggressive disease with poor survival. According to the cBioportal database, *δ-catenin* gene alterations including amplification and mutations were found in 20% (16 out of 81) of patients with NEN PCa (Fig. 2D). Since deep sequencing identified less SNPs compared with the targeted Sanger sequencing demonstrated in our previous studies,[10] it is likely that *δ-catenin* gene mutations are underestimated as well in the cBioportal database. Taken together, these studies show that *δ-catenin* undergoes extensive gene alterations in metastatic PCa and may acquire new functions that are not predicted in its original full-length protein.

Wildtype and mutant forms of δ-catenin elicit non-overlapping interactomes involved in distinct biological processes

To investigate the differential effects of full-length δ-catenin and the mutant δ-catenin with carboxyl terminal truncation on PCa cells, Rv1-M6 cells were sorted into two groups. The full-length δ-catenin group showed junctional distribution (JAD) whereas the mutant δ-catenin group displayed mostly cytoplasmic distribution (CAD). Proteomic analysis of proteins isolated from co-immunoprecipitation of δ-catenin variants in JAD and CAD cells revealed 109 and 112 hits, respectively. Only 36 hits were shared (Fig. 2E). Only 39 out of 109 in JAD/WT, 47 out of 112 in CAD/truncated, and 32 out of 36 in both were identified/verified genes. These genes were subjected to enrichment and network analysis.

To identify the potential changes to signaling associated with mutant δ-catenin, we examined the biological processes using network analysis using BiNGO. Biological processes related to 33 out of 39 hits in JAD/WT, 36 out of 47 hits in CAD/truncated, and 30 out of 32 hits in both were statistically significant ($p < 0.05$). Altogether, the 99 genes were categorized into 902 biological processes (Fig. 2F and Supp. Table II). Interestingly, 97 biological processes were specific for the JAD/WT group while 199 were specific for the CAD/truncated group. The CAD/truncated group uniquely activated several biological processes related to cytokine regulation, steroid receptor signaling, hormone response, and actin-myosin contraction (Supp. Table II). Alternatively, the JAD/truncated mutant lost 97 processes/functions found only in the WT group such as negative regulation of transcription, pH regulation, and NF-κB regulation (Supp. Table II). Meanwhile proteomic and enrichment analysis of δ-catenin and cytoskeletal proteins such as tubulin and actin confirmed their involvement in well-established biological processes such as cell-cell adhesion, microtubule-based process, and organelle organization, respectively (Supp. Table III). This data suggests that the δ-catenin JAD distribution may interact with distinct signaling networks when compared with that of the mutant δ-catenin CAD distribution which may have gained functions by interacting with non-junctional protein signaling networks.

Differential δ-catenin subcellular distribution corresponds to the different fate of E-cadherin/p120^{ctn} and influences the interactions of p120^{ctn} with Rho GTPases

To investigate how JAD and CAD δ-catenin may potentially control cell functions, we first focused on a well-established interaction between δ-catenin and cell adhesion. Since δ-catenin and p120^{ctn} bind to the same juxtamembrane domain on E-cadherin but showed an inverse expression pattern in PCa development,[3] we applied the pixel density index of junction to cytoplasm (Jun/Cyto) ratio to analyze the potential contribution of regional δ-catenin expression to E-cadherin and p120^{ctn} distribution. The higher the index the stronger the expression at cell-cell junction.

Figure 3A shows that E-cadherin index of Jun/Cyto is higher when δ-catenin distributed at cell-cell junction (JAD) than when δ-catenin presented CAD expression pattern in Rv1-M6 cells. The p120^{ctn} index of Jun/Cyto showed a similar trend to that of E-cadherin index (Fig. 3A). These results are consistent with the ability of JAD δ-catenin to stabilize E-cadherin at the cell-cell junction while CAD δ-catenin is associated with the loss of this function on E-cadherin cell-cell junction but may gain new functions in the cytoplasm.

Rho GTPases are molecular switch proteins that are classically controlled by regulators and phosphorylation.[20] Expression of p120^{ctn} increases activity of Cdc42 and Rac1, and decreases RhoA activity.[21,22] Overexpression of δ-catenin also donwregulates RhoA.[5] To determine whether different subcellular δ-catenin distribution results in changes in Rho GTPase activity in PCa cells, we analyzed fluorescent pixel intensity of phosphorylated RhoA, Rac1, and Cdc42 in association with δ-catenin JAD and CAD (Fig. 3B). δ-Catenin CAD increased phosphorylated RhoA and Rac1 indicating stronger inhibition of RhoA and Rac1 compared to δ-catenin JAD. On the other hand, δ-catenin CAD reduced phosphorylated Cdc42 indicating stronger activation of Cdc42 compared to δ-catenin JAD.

As δ-catenin and p120^{ctn} are both modulators of Rho GTPases, we investigated whether δ-catenin overexpression altered the interactions between Rho GTPases and p120^{ctn}. Overexpression of δ-catenin led to an increase in phosphorylated Rac1 and a decrease in phosphorylated Cdc42 (Fig. 3C) as observed in our pixel density results. To determine if δ-catenin overexpression directly altered δ-catenin and Rho GTPase interactions, we performed co-immunoprecipitation. Pull-down of Rho GTPases and probing for δ-catenin revealed increased interaction of mutant δ-catenin with Cdc42. However, co-immunoprecipitation indicated minimal direct interactions of δ-catenin with RhoA and Rac1 (Fig. 3D). Therefore, δ-catenin alteration of the phosphorylation of these RhoA and Rac1 may be indirect. On the other hand, overexpression of δ-catenin decreased the interaction of p120^{ctn} with RhoA and increased p120^{ctn} interaction with Cdc42 (Fig. 3E).

Knockdown of p120^{ctn} altered Rho-GTPase function/activation/phosphorylation in δ-catenin overexpressing CWR22Rv1 cells

It is well known that p120^{ctn} regulates actin cytoskeleton organization and cell motility through Rho family GTPases,[21] balancing between adhesive and motile phenotypes. Since δ-catenin belongs to the p120^{ctn} subfamily of the β-catenin/armadillo superfamily, different

cell proliferative and migratory behavior due to different δ-catenin distribution and Rho GTPases may be influenced by competition with p120^{ctn} localization.

We knocked down p120^{ctn} expression in CWR22Rv1 with δ-catenin overexpression (Rv1-M6) cells to determine its effects on δ-catenin interaction with Rho family small GTPases. Knockdown of p120^{ctn} decreased δ-catenin protein expression in Rv1-M6 cells and did not appear to affect total RhoA and Cdc42 protein level. However, we observed an increase in phosphorylation of RhoA and Cdc42 following p120^{ctn} knockdown when compared to Rv1-M6 cells (Fig. 3F). δ-Catenin expression (Rv1-M6) slightly decreased pCdc42 level when compared to C2 cells. Knockdown of p120^{ctn} in Rv1-M6 cells resulted in increased pCdc42 level. These results indicate that δ-catenin can inhibit RhoA function in a p120^{ctn}-independent manner. Meanwhile, p120^{ctn} positively regulates Cdc42. This is in line with our findings in Figure 3 such that p120^{ctn} directly binds to Cdc42 (Fig. 3E) and results in an increase in pCdc42 level (Fig. 3F). Knockdown of p120^{ctn} in Rv1-M6 cells resulted in increased pCdc42 level. Taken together, after p120^{ctn} knockdown, the net effect of δ-catenin expression was still the inhibition of RhoA while its effect on activating Cdc42 reversed to inhibition.

Differential δ-catenin subcellular distribution determines different cell fate and behavior and influences growth factor responses of PCa cells

It is well known that FGFs stimulate the proliferation, migration, and differentiation of epithelial cells.[23] In addition, recent studies showed that androgen receptor pathway-independent PCa is sustained through FGF signaling.[15] Therefore, we examined the cell behavior of Rv1-M6 cells with δ-catenin JAD or CAD in response to treatment with bFGF using time-lapse video light microscopy (Fig. 4A and 4B).

In the same 24-hour recording period, Rv1-M6 cells with δ-catenin JAD expression showed an increased cell number when compared to that of CAD expression (Fig. 4A and 4C, -bFGF). Interestingly, treatment with bFGF resulted in decreased cell number in JAD compared to JAD without bFGF treatment (Fig. 4C JAD -bFGF and +bFGF). The treatment with bFGF did not increase cell number in CAD (Fig. 4C, CAD -bFGF and +bFGF), either. However, following bFGF stimulation, cells with δ-catenin CAD expression were visibly more motile in that many of them moved in and out of focus and were displaced during the 24-hour recording period (Fig 4B, CAD+bFGF; Fig 4D, CAD). The enhanced motile behavior was exemplified in δ-catenin CAD cells moving away from the initial cell cluster (Fig 4B, CAD+bFGF; compare 0hr with 24hr: asterisks). In contrary, δ-catenin JAD cells remained in focus as sheet of cell clusters during the recording period (Fig 4B, JAD +bFGF), and fewer cells were displaced (Fig 4D, JAD).

To further discern the roles of δ-catenin on FGF-stimulated cell signaling events, we studied downstream MAP kinase phosphorylation signaling. We examined p38 and p44/42 MAPK expression and phosphorylation in Rv1 and PC3 cells with overexpressed mutant (R3 and T4) and full-length (M6) δ-catenin (Fig. 4E and 4F). In all Rv1 cells, there was no significant response of p-p38 to bFGF stimulation. Meanwhile, p-p44/42 was activated in all Rv1 cells (C2, R3, and M6) after 30 minutes of bFGF stimulation. The truncation mutant Rv1-R3 cells showed the strongest molecular weight shift in pan-ERK expression

(Fig. 4E, Rv1-R3 pan-ERK). After overnight treatment of bFGF, MAPK expression and phosphorylation decreased, although p-p44/42 MAPK was still detected in Rv1-R3 and Rv1-M6 cells (Fig 4E, p-p44/42 MAPK).

Transfected PC3 cells showed significant changes in p-p38 levels after stimulation with bFGF (Fig 4F). PC3-R3 and PC3-T4 cells showed a significant increase in p-p38 levels 30 min after bFGF stimulation. Moreover, p-p38 levels were sustained even after overnight treatment. In contrast, the parental PC3-C2 cells showed only a moderate increase in p-p38 levels following 30 min activation with bFGF. In addition, p-p38 levels in PC3-C2 cells dropped sharply after overnight stimulation with bFGF. Thus, overexpression of mutant δ-catenin promotes and prolongs bFGF-p38 signaling. Meanwhile, stimulation of the PC3 cells with bFGF increased p-p44/42 levels in all cells. No significant changes were detected in pan-ERK levels in PC3 cells with or without δ-catenin overexpression.

To gain additional insights into the functions of δ-catenin mutation in PCa progression *in vivo*, we generated Myc/δ-catenin mutant mice.[10,24] ARR_2PB-Myc transgenic mice were further cross-bred with δ-catenin heterozygous (δ-cat$^{+/-}$) mutant mice to obtain Myc with δ-catenin homozygous mutation (Myc/δ$^{-/-}$) in which δ-catenin expresses as a truncated protein lacking the carboxyl terminus and the entire armadillo domain (Supp. Fig. 3).[10,25] This mutation mimics those seen in human PCa and CWR22Rv1-M6 PCa xenograft cells that demonstrated AAD/CAD distribution (Fig. 1).

The increased MAPK signaling was also observed in transgenic mice expressing Myc/δ-catenin (Fig. 4G). The expression of mutant δ-catenin increased p-p38 level (Fig 4G, Myc/δ$^{-/-}$). While the expression of WT δ-catenin increased p44/42 MAPK level (Fig 4G, Myc/δ$^{+/+}$), expression of mutant δ-catenin resulted in the decrease of p-p44/42 (Fig 4G, Myc/δ$^{-/-}$). Therefore, expression of WT and mutant δ-catenin altered MAPK signaling in both PCa cell culture and transgenic mice expressing oncogenic *Myc*.

Myc/δ-catenin mutant mice promote prostate tumor development in a mutation dependent manner

We further examined the histopathological changes in three different genotypes (Myc/δ$^{+/+}$, Myc/δ$^{+/-}$, and Myc/δ$^{-/-}$) compared to WT mice at 6 weeks (Fig. 5A) and 6 months (Fig. 5B) of ages. At 6 weeks, the DLP and VP of Myc/δ$^{+/+}$, Myc/δ$^{+/-}$, and Myc/δ$^{-/-}$ prostates exhibited multilayering of cells partially filling the lumen, characteristics of mPIN lesions (Fig. 5A). In addition to multi-layering of cells, the changes in Myc/δ$^{+/-}$ and Myc/δ$^{-/-}$ mutant mice included prominent nucleoli, nuclear shape variability, and intraepithelial space formation (Fig. 5A, b–d, f–h, j–l, and n–p, asterisks). Additionally, Myc/δ-catenin mutant mice displayed the loss of polarity, which can be characterized by a variation in the location of nuclei within the mPIN cells rather than basally located nuclei observed in wild-type animals (indicated by arrows). Striking differences were observed in the prostates of Myc/δ$^{+/+}$, Myc/δ$^{+/-}$, and Myc/δ$^{-/-}$ at 6 months of age (Fig. 5B). Myc/δ$^{-/-}$ mice progressed to develop invasive adenocarcinoma (Fig. 5B, p) whereas Myc/δ$^{+/+}$ and Myc/δ$^{+/-}$ mice continued to exhibit mPIN at the same time point (Fig. 5B, f–g and n–o). These findings indicate that a homozygous mutation in δ-catenin resulting in its truncation exacerbates prostate tumor progression in Myc transgenic mice.

δ-Catenin mutations enhance β-catenin, Myc, and HIF-1α expression in Myc/δ-catenin mutant mice

Many studies have primarily compared δ-catenin to other p120^{ctn} subfamily members.[26] Fewer studies have directly addressed the shared functional properties between Wnt modulator β-catenin and δ-catenin.[27,28] Kim et al (2012) reported δ-catenin mediates nuclear accumulation of β-catenin, resulting in the transcription of genes involved in cell cycle (e.g., cyclin D1), and cell proliferation (e.g., Myc).[29] In addition, we recently reported that δ-catenin mutations increased β-catenin translocation to the nucleus and HIF-1α expression in PCa xenograft cells.[10] Thus, aberrant signaling in this pathway is associated with overproliferation.[13] Therefore, we further investigated what effects δ-catenin mutations exert on Myc/δ-catenin mutant PCa mouse model by engaging β-catenin-mediated oncogenic signaling pathway (Fig. 6).

Western blot analysis of 6-month old mice revealed significantly increased β-catenin expression, which was correlated with marked reduction in phosphorylated β-catenin in mutant Myc/$\delta^{-/-}$ mice (Fig. 6A and B, * $p<0.01$, relative to wild type and Δ $p<0.01$, relative to Myc/$\delta^{+/+}$). Phosphorylated β-catenin is indicative of targeted-β-catenin for ubiquitin-dependent degradation in the proteasome. These results suggested that β-catenin is stabilized in cytoplasm in Myc/$\delta^{-/-}$ mice. Furthermore, Myc, a downstream effector of Wnt/β-catenin signaling pathway, increased dramatically, corresponding with β-catenin expression (Fig. 6A). Quantification of protein density in Fig. 6C confirmed the visual comparison and demonstrated mutant δ-catenin not only significantly increased Myc in Myc/$\delta^{-/-}$ as compared to wild type (* $p<0.01$), but also to Myc/$\delta^{+/+}$ and Myc/$\delta^{+/-}$ (Δ $p<0.01$). These findings support that mutations of δ-catenin facilitated tumorigenesis by altering β-catenin and Myc protein levels, leading to mouse prostate tumor growth.

HIF-1α upregulates the expression of glucose transporters and most of the glycolytic enzymes under hypoxia, increasing the capacity of the cell to carry out glycolysis.[30–32] In addition, HIF-1α cooperates with Myc to enhance the expression of shared targets in the glycolytic pathway.[33–35] Our earlier study showed that δ-catenin mutations increased HIF-1a expression in cultured PCa cells. Here, we further found that HIF-1α protein expression was minimal in wild type mice (Fig. 6A). However, HIF-1α was significantly increased, which was correlated to a dosage of δ-catenin mutations and Myc protein expression in mutant mice (Fig. 6A and D, * $p<0.01$, relative to wild type and Δ $p<0.01$, relative to Myc/$\delta^{+/+}$). These findings further support the hypothesis that the *Myc* oncogene, besides its-well documented role in controlling cell proliferation, alters the metabolic phenotype in favoring tumorigenesis.

δ-Catenin mutations promote a dramatic increase in cells overexpressing Myc in Myc/δ-catenin mutant mice

Myc overexpression is reported to localize within luminal epithelial cells correlated with the onset of morphological transformation of mPIN lesions in Myc transgenic mouse models.[36] As depicted in Fig.6E, immunofluorescent analysis revealed a distinct pattern of Myc expression. Not all prostatic epithelial cells showed positive anti-Myc staining. Myc/$\delta^{+/+}$ and Myc/$\delta^{+/-}$, with a well-defined luminal-basal compartment, demonstrated anti-

Myc positive cells being localized predominantly in luminal epithelial cells (white asterisks indicate lumina), whereas Myc/$\delta^{-/-}$ cells staining positively for Myc were beyond luminal epithelial cells and located all over tumor lesions. Additionally, wild-type prostates were completely negative for anti-Myc staining. We also observed that number of cells expressing Myc was significantly increased in Myc/$\delta^{-/-}$ (Fig 6F, * $p<0.01$, relative to wild type and Δ $p<0.05$, relative to Myc/$\delta^{+/+}$). These findings also supported that Myc/$\delta^{-/-}$ promoted prostatic tumorigenesis and progression.

The morphological and functional changes in the nuclei are widely observed in cancer tissues and directly related to the rate of proliferative cancer cells. We hypothesize that δ-catenin mutants lead to an alteration of nuclei in Myc transgenic mice. We determined the nuclear area as identified by Hoechst-stained nuclei and Myc expressing cells (with the exception of WT mouse prostate section which was anti-Myc negative). The results showed that relative nuclear area of Myc/$\delta^{-/-}$ was approximately 2.9- and 1.4-fold greater than WT and Myc/$\delta^{+/+}$, respectively (Fig. 6G).

DISCUSSION

Genomic aberrations are well recognized as cancer drivers and dictate the direction of cancer development.[13] In this report, we demonstrated how genetic mutations contribute to the functional heterogeneity of cancer cells using the Wnt/β-catenin modulator δ-catenin as a model example (Fig. 7). We anticipate that the gain-of-novel functions (or neomorphism) due to genetic alterations would be widespread across human genome landscape.[2,9,11]

Inside the tumor where δ-catenin mainly located at cell-cell junction, it co-localized with E-cadherin and $p120^{ctn}$, and promoted cell proliferation. This can be simulated in cultured PCa cells in which δ-catenin JAD cells grew faster than CAD cells. With rapid tumor growth, cancer cells inside the tumor mass became deprived of nutrition, such as oxygen and glucose supplies. It is well known that cancer cells deregulate expression of many genes during transformation. Some genes, when expressed highly, can be harmful for overall tumor growth if the nutrition supplies cannot match the demand of rapid growth. Our previous studies identified that δ-catenin (*CTNND2*) gene displays somatic mutations for cell survival and metabolic adaptation during densely packed tumorigenesis.[10]

In addition, at the border of the tumor mass, δ-catenin may have high propensity for mutagenesis to promote cancer progression accompanied by developing androgen independence. This notion can be simulated in cultured PCa cells, in which δ-catenin CAD cells grew faster than JAD cells when treated with bFGF, a growth factor signaling pathway known to be used by PCa cells to bypass androgen dependence.[15] δ-Catenin lacking carboxyl terminus loses the function of stabilizing cadherin-mediated cell-cell junction. In this scenario, mutant δ-catenin is dissociated from cell membrane and re-localized to the cytoplasm. In turn, $p120^{ctn}$ and E-cadherin are also re-located from cell-cell junction to the cytoplasm and are down-regulated during tumor progression. Cytoplasmic mutant δ-catenin and $p120^{ctn}$ as well as its downregulation inhibit RhoA and activate Rac1/Cdc42 thereby promoting cell motility and invasion.[37–42] Therefore, PCa cells with δ-catenin mutations increased potential to spread and migrate. Indeed, when we treated cells with bFGF, CAD

cells became more motile. This is consistent with the roles of Rho family small-GTPase in cancer progression. Moreover, we presented data that further implicates the role of δ-catenin in Myc signaling which shows altered p38 and p44/42 phosphorylation.

Examination of Sanger cancer gene mutation database revealed remarkable variations in *δ-catenin* coding and non-coding regions in many cancer types including PCa. The Cancer Genome Atlas (TCGA) project also demonstrated the wealth of *δ-catenin* gene variants including SNPs, mutations, deletions as well as gene fusion.[41] These data from unbiased genome landscape corroborated with our targeted gene sequencing results. Not only have we found that *δ-catenin* displayed increased sequence variations in primary prostatic adenocarcinoma,[10] but we have also demonstrated in this study that *δ-catenin* mutations are widespread in the advanced metastatic tissues such as lymph node metastasis and neuroendocrine transdifferentiated prostate tumors.

These studies raised a question about the fate of the mutant δ-catenin and the roles of the mutations in cancer evolution. If the mutations are the products of selection for cancer progression, then would there be increased mutant δ-catenin in the late stage of cancer and less full-length δ-catenin in the end? In some cancer types, it is reported that δ-catenin exists as a protein with sizes much smaller than the predicted full-length protein.[42,43] Therefore, it may be true that δ-catenin accommodated a mechanism to eliminate the full-length protein early in some cancer types. On the other hand, we have not confirmed that all PCa cells lost the full-length protein. At least in some cancer cells, the full-length proteins are retained. Therefore, it is possible that the roles of δ-catenin mutants are stage- and subcellular location-dependent in cancer progression.

Altogether, we present data that elucidates the potential role of CAD/mutant δ-catenin in PCa (Fig. 7). Overexpression of CAD/mutant δ-catenin altered Rho GTPase activation and increased the expression of HIF-1α, β-catenin, and Myc. CAD/mutant δ-catenin also appeared to alter MAPK signaling differentially through p44/42 (CWR22Rv1 tumor) or p38 (PC3 metastasis) , but direct interactions remain to be determined (Fig. 7, orange dashed arrow). Following stimulation with bFGF, we observed activation of MAPK-myc signaling *in vivo* (Fig. 7 black arrows). However, the direct interactions of FGFR and CAD/mutant δ-catenin is unclear at present (Fig. 7, dashed black arrow).

δ-Catenin is not the only gene that gained novel functions by mutagenesis for promoting cancer. The neomorph concept was first proposed in Drosophila by the Nobel laureate H. J. Muller in 1932. In recent years, neomorphic mutations became increasingly associated with cancer progression.[11] IDH1 and IDH2, PI3K, PTEN, TP53, MYOD1, and YY1, all of which showed neomorphic phenotypes. In addition, not only the coding regions of the genes but also the non-coding elements of genes can also be altered by duplications, deletions, and fusions.[44] Acquired and/or novel gene re-arrangements can either be induced from therapy or be tumor progression driven such as the dichotomy of CDK12 amplifications and inactivation.[45] Recognizing that novel gain-of-functions can be introduced in both oncogenes and tumor suppressors has important implications when designing cancer therapeutics. As discussed by Takiar et al (2017), the unanticipated phenotypic effects elicited by neomorphic mutations of oncogenes and tumor suppressor genes indicated

that tumors with the neomorphic mutations may not respond to the cancer therapies currently designed to target the wild type proteins. Consequently, an effective cancer treatment strategy should consider the functional impacts of each genomic aberrations to be targeted.[46,47] Our current studies open the door for further interrogating other genes in the same way and screening small molecules that can specifically target the mutant cells within the tumor.

MATERIALS AND METHODS

Antibodies and reagents

Mouse antibodies against E-cadherin, p120ctn, δ-catenin or total-Rac were obtained from BD transduction Lab. Rabbit antibody against total-RhoA (polyclonal) was obtained from Cytoskeleton, and total-Cdc42 was from Santa Cruz. Rabbit polyclonal anti-phosphorylated-RhoA (serine188) and anti-phosphorylated Rac1/Cdc42 (Serine71) were obtained from Millipore. Monoclonal anti-GAPDH was from EMD Science. Phosphorylated antibodies: 1:1000 phospho-p38 MAPK (Rabbit, Cell Signaling Tech), 1:2000 phospho-p42/44 MAPK (Rabbit, Cell Signaling Tech), 1:1000 phospho-SAPK/JNK (Rabbit, Cell Signaling Tech). Total antibodies: 1:500 p38α (F-9) (Mouse, Santa Cruz), 1:500 pan-ERK (Mouse, Transduction Laboratories), 1:500 ERK2 (C-14) (Rabbit, Santa Cruz), 1:500 JNK (D-2) (Mouse, Santa Cruz). Control antibodies: 1:2000 GAPDH (Mouse, Calbiochem), 1:1000 Histone H3 (Rabbit, Cell Signaling Tech), 1:1000 α-Tubulin (Mouse, Sigma). Sepharose beads conjugated anti-RhoA and sepharose beads conjugated anti-Cdc42 were from Santa Cruz Biotech. All other chemicals were form Sigma unless indicated otherwise. Recombinant Basic Fibroblast Growth Factor (bFGF) was from Biosource.

Tissue for protein assay (Western blot and IP)

Human primary prostatic tumor tissues and metastatic lymph nodes were collected according to the Institutional Research Board protocols with informed consent obtained from all subjects. Tissues for protein assay were lysed in RIPA buffer (1% Triton X-100, 0.5% Deoxycholic Acid, 0.2% SDS, 150mM sodium chloride, 2mM EDTA) with complete protease inhibitor cocktail tablets (Roche, Germany) and pepstatin A. After removing debris by centrifugation, protein concentration was determined using BCA method. Some cell lysates were immunoprecipitated using anti-RhoA or anti-Cdc42 conjugated sepharose beads, or anti-Rac1 antibody followed with Protein G beads and then Western blotted with anti-phosphorylated RhoA (serine188) or anti-phosphorylated Rac1/Cdc42 (Serine71).

The proteins separated by SDS-PAGE were transferred to the nitrocellulose membrane (Optitran, Germany) for Western blot analyses. The primary antibodies used were against the following antigens: E-cadherin, p120ctn, δ-catenin, phosphorylated-RhoA, phosphorylated-Rac1/Cdc42 and GAPDH. After incubation in appropriate secondary antibodies, the membranes were developed with ECL detection reagents. Protein amount were semi-quantified in triplicates using Quantity One (BioRad). Statistics analyses were performed and the p-values were assigned with the confidence levels set at 95%.

H&E and Immunohistochemistry

For human prostate tissue H&E staining, 5μm serial tissue sections of paraformaldehyde-fixed, paraffin-embedded blocks were deparaffinized and rehydrated; endogenous peroxidase was blocked by incubation with hydrogen peroxide. The sections were stained with H&E staining followed the standard protocol and observed under microscope.
The sections were also immunostained using mouse anti-δ-catenin (1:100), mouse anti-E-cadherin (1:100) and mouse anti-p120 (1:100) followed by streptavidin-biotin peroxidase method for detection. The immunostaining was done in Dako Autostainer (Carpinteria, CA) according to the manufacture instruction.

Cell culture and cell sorting

Transfection of CWR22-Rv1, PC3, and LNCaP PCa cells and sorting were conducted as previously described.[10] Briefly, PCa cells stably transfected with δ-catenin (named as Rv1-M6, PC3-T4, and LNCaP-M6) or GFP vector alone (named as Rv1-C2, PC3-C2, and LNCAP-C2) were grown in RPMI1640 medium with 0.25% Gentamicin (G418) (Gibco). While PC3-T4 cells represented the PC3 cells transfected with full-length δ-catenin, they were rapidly converted to stable PC3-R3 cells displaying carboxyl terminal truncation. On the other hand, Rv1-M6 cells were able to maintain full length δ-catenin expression when cultured with optimal condition. All cells were incubated at 37°C in 5% CO2 environment. After sorting, cells in different groups were collected separately for protein assay validation. All experiments were repeated at least three times.

Immunofluorescent light microscopy

Rv1, LNCaP, and PC3 cells with varying expression of δ-catenin were plated on the coverslips and fixed in 4% paraformaldehyde. Following permeabilization in 0.2–0.5% Triton X-100, the cells were stained using mouse anti-E-cadherin, anti-p120ctn, anti-phosphorylated Rac1/Cdc42 or rabbit anti-phosphorylated RhoA. The cells were then incubated with the appropriate Cy3 conjugated secondary antibodies. The nuclei of the cells were stained with Hoechst 33258. The coverslips were mounted on slides using Anti-Fade medium (Invitrogen) and photographed under the Zeiss Axiovert inverted fluorescent microscope or Nikon's Stochastic Optical Reconstruction Microscopy (N-STORM). Immunofluorescent density analyses were performed using a MetaMorph 4.6 imaging software system (Universal Imaging Corp., West Chester, PA). All data was presented as Mean±SEM and statistically evaluated with t-test. The confidence level was set at 95%.

Immunoprecipitation and Western blot with ECL detection

Cells for protein assay were lysed in RIPA buffer with complete protease inhibitor cocktail tablets (Roche, Germany) and pepstatin A. After removing cell debris by centrifugation, protein concentration was determined using BCA method. Some cell lysates were immunoprecipitated using anti-RhoA or anti-Cdc42 conjugated sepharose beads, or anti-Rac1 antibody followed with Protein G beads and then Western blotted with anti-phosphorylated RhoA (serine 188) or anti-phosphorylated Rac1/Cdc42 (Serine 71).

The proteins separated by SDS-PAGE were transferred to the nitrocellulose membrane (Optitran, Germany) for Western blot analyses. The primary antibodies used were against the following antigens: E-cadherin, p120ctn, δ-catenin, phosphorylated-RhoA, phosphorylated Rac1/Cdc42 and GAPDH. After incubation in appropriate secondary antibodies, the membranes were developed with ECL detection reagents. Protein amount were semi-quantified in triplicates using Quantity One (BioRad). Statistical analyses were performed and the p-values were assigned with the confidence levels set at 95%.

Interactome analysis

CWR22Rv-1 cells stably expressing wild type or mutant δ-catenin were lysed in HEPES buffer containing octyl glucoside.[48] 46 Wild type or mutant δ-catenin were immunoprecipitated and processed for protein sequence identification using MALDI-TOF/TOF. Data was searched against a publicly available protein database using Mascot search engine. Data was processed in Protein Pilot. Enrichment analysis was performed with BINGO 2.44 in Cytoscape 2.81 software (www.cytoscape.org). For statistical analysis of enrichment data created with BINGO/Cytoscape hypergeometric tests were performed and corrected by Benjamini & Hochberg False Discovery Rate (FDR) correction at a significance level of 0.05.[49]

Time-lapse imaging

Rv1-M6 and Rv1-C2 cells with different GFP-δ-catenin expression patterns (JAD or CAD) were recorded by time-lapse light microscopy as described with some modifications.[50,51] Cells were also treated with bFGF to examine the different responses of GFP-δ-cateninJAD and CAD. bFGF (10ng/ml) was used to treat the cell for 24 hours under the serum-free media. Continuous video microscopy of Rv1-M6 and Rv1-C2 cells was performed using the WaferGen Smart Slide System (WaferGen, Incorporated, Freemont, CA). The cells were plated on a WaferGen Smart Slide 100 and maintained at 37°C, with the lid at 39°C to prevent condensation. CO_2 was maintained at 5% over the course of the experiment. Images were obtained at time-lapse mode using a Zeiss Axiovert microscope (Carl Zeiss), and the camera was set up to record a picture of the cell every 30 minutes for 24 hours using MetaMorph (4.6) software.

siRNA against p120^{ctn}

Rv1-M6 and Rv1-C2 cells were transfected using Lipofectamine Plus reagent (Invitrogen) according to the manufacturer's instructions. For *p120^{ctn}* knockdown experiments, specific siRNAs directed against human *p120^{ctn}* nucleotide sequences were obtained from Darmacon Technologies (USA). The ON-target plus SMARTpool siRNA oligonucleotide sequences were as follows: GGAAUGUGAUGGUUUAGUU, UAGCUGACCUCCUGACUAA, GGACCUUACUGAAGUU-AUU, GAGUGAAGCUCGCCGGAAA. A scramble siRNA was used as control.

Cell growth assay

Cells were harvested after trypsinzation and resuspended in complete media at 1.0×10^5 cells per well in 12-well plates. At the indicated times after plating, cells were trypsinized, mixed

with trypan blue at a 1:1 dilution, and counted using an automated cell counter (Invitrogen, Countess). All experiments were performed in triplicate. Data are expressed as mean±SEM, and a growth curve was drawn.

Analysis of δ-catenin gene variations in human PCa tissue

PCR analysis was used to amplify *δ-catenin* exon sequence at Genomic DNA level in prostate cancer cases. The PCR primers used for detection of *δ-catenin* DNA

a. Genomic DNA extraction form tissue—Genomic DNA were extracted from fresh tissue using DNeasy Tissue Kit (QIAGEN Science, Maryland) or from Paraffin embedded primary prostatic adenocarcinoma samples and non-cancer prostate tissues after LCM using Pico Pure DNA Extraction kit (Arcturus Bioscience, Mountain View, CA).

b. PCR amplification of δ-catenin gene—PCR analysis was used to amplify *δ-catenin* exon sequence at Genomic DNA level in PCa cases. The PCR primers used for detection of *δ-catenin* DNA sequencing are listed in supplemental materials.

c. PCR products sequence analysis—Directly purified PCR products using QIAquick PCR Purification Kit (QIAGEN Science, Maryland) and send to sequence. The DNA sequences of amplified PCR fragments obtained from PCa tissues and the matched adjacent normal prostate cells were compared to human *δ-catenin* DNA sequence as reference published in the NCBI database using BLAST Program.

δ-Catenin mutant and Myc transgenic mice

The Myc/δ-Catenin compound transgenic mice were generated as previously described.[10] The animals were housed under pathogen-free conditions according to the guidelines of East Carolina University Animal Use Protocol. Transgenic animals were analyzed with at least 6 littermates, and both males and females were considered. Animals at 6 weeks and 6 months were analyzed. If the animal age was beyond one week from the 6-week experiments or two weeks from the 6-month experiments, they would be excluded from the analysis. Randomization was not pre-adopted and the experiments were performed with partial blinded analyses.

Supplementary Material

Refer to Web version on PubMed Central for supplementary material.

ACKNOWLEDGEMENTS

We thank George W. Lanford and William Guiler for technical assistance. This work was supported in part by grants from USA National Cancer Institute CA111891 (QL), CA165202 (QL), the Harriet and John Wooten Foundation for Alzheimer's and Neurodegenerative Diseases Research (QL), and Chinese Beijing Natural Science Foundation 7172068 (YGJ). This research is based in part upon work conducted using the UNC Proteomics Core Facility, which is supported in part by USA National Cancer Institute P30 CA016086 Cancer Center Core Support Grant to the UNC Lineberger Comprehensive Cancer Center.

REFERENCES

1. Chaffer CL, San Juan BP, Lim E, Weinberg RA. EMT, cell plasticity and metastasis. Cancer Metastasis Rev 2016; 35: 645–654. [PubMed: 27878502]
2. Zhang Y, Weinberg RA. Epithelial-to-mesenchymal transition in cancer: complexity and opportunities. Front Med 2018; 12: 361–373. [PubMed: 30043221]
3. Lu Q δ-Catenin dysregulation in cancer: interactions with E-cadherin and beyond. J Pathol 2010; 222: 119–123. [PubMed: 20715154]
4. Lu Q, Paredes M, Medina M, Zhou J, Cavallo R, Peifer M et al. delta-catenin, an adhesive junction-associated protein which promotes cell scattering. J Cell Biol 1999; 144: 519–532. [PubMed: 9971746]
5. Kim K, Sirota A, Chen Yh Y, Jones SB, Dudek R, Lanford GW et al. Dendrite-like process formation and cytoskeletal remodeling regulated by delta-catenin expression. Exp Cell Res 2002; 275: 171–184. [PubMed: 11969288]
6. Westbrook TF, Martin ES, Schlabach MR, Leng Y, Liang AC, Feng B et al. A genetic screen for candidate tumor suppressors identifies REST. Cell 2005; 121: 837–848. [PubMed: 15960972]
7. Zeng Y, Abdallah A, Lu J-P, Wang T, Chen Y-H, Terrian DM et al. delta-Catenin promotes prostate cancer cell growth and progression by altering cell cycle and survival gene profiles. Mol Cancer 2009; 8: 19. [PubMed: 19284555]
8. Fang Y, Li Z, Wang X, Zhang S. Expression and biological role of δ-catenin in human ovarian cancer. J Cancer Res Clin Oncol 2012; 138: 1769–1776. [PubMed: 22699932]
9. Zhang J, Chen Y-H, Lu Q. Pro-oncogenic and anti-oncogenic pathways: opportunities and challenges of cancer therapy. Future Oncol 2010; 6: 587–603. [PubMed: 20373871]
10. Nopparat J, Zhang J, Lu J-P, Chen Y-H, Zheng D, Neufer PD et al. δ-Catenin, a Wnt/β-catenin modulator, reveals inducible mutagenesis promoting cancer cell survival adaptation and metabolic reprogramming. Oncogene 2015; 34: 1542–1552. [PubMed: 24727894]
11. Takiar V, Ip CKM, Gao M, Mills GB, Cheung LWT. Neomorphic mutations create therapeutic challenges in cancer. Oncogene 2017; 36: 1607–1618. [PubMed: 27841866]
12. Wolf A, Keil R, Götzl O, Mun A, Schwarze K, Lederer M et al. The armadillo protein p0071 regulates Rho signalling during cytokinesis. Nat Cell Biol 2006; 8: 1432–1440. [PubMed: 17115030]
13. Hanahan D, Weinberg RA. Hallmarks of cancer: the next generation. Cell 2011; 144: 646–674. [PubMed: 21376230]
14. Swanton C Intratumor heterogeneity: evolution through space and time. Cancer Res 2012; 72: 4875–4882. [PubMed: 23002210]
15. Bluemn EG, Coleman IM, Lucas JM, Coleman RT, Hernandez-Lopez S, Tharakan R et al. Androgen Receptor Pathway-Independent Prostate Cancer Is Sustained through FGF Signaling. Cancer Cell 2017; 32: 474–489.e6. [PubMed: 29017058]
16. Lu Q, Dobbs LJ, Gregory CW, Lanford GW, Revelo MP, Shappell S et al. Increased expression of delta-catenin/neural plakophilin-related armadillo protein is associated with the down-regulation and redistribution of E-cadherin and p120ctn in human prostate cancer. Hum Pathol 2005; 36: 1037–1048. [PubMed: 16226102]
17. Tai S, Sun Y, Squires JM, Zhang H, Oh WK, Liang C-Z et al. PC3 Is a Cell Line Characteristic of Prostatic Small Cell Carcinoma. Prostate 2011; 71: 1668–1679. [PubMed: 21432867]
18. Zheng J-Y, Yu D, Foroohar M, Ko E, Chan J, Kim N et al. Regulation of the Expression of the Prostate-specific Antigen by Claudin-7. J Membrane Biol 2003; 194: 187–197. [PubMed: 14502431]
19. Suhovskih AV, Kashuba VI, Klein G, Grigorieva EV. Prostate cancer cells specifically reorganize epithelial cell-fibroblast communication through proteoglycan and junction pathways. Cell Adh Migr 2016; 11: 39–53. [PubMed: 27111714]
20. Olson MF. Rho GTPases, their post-translational modifications, disease-associated mutations and pharmacological inhibitors. Small GTPases 2016; 9: 203–215. [PubMed: 27548350]

21. Anastasiadis PZ, Reynolds AB. Regulation of Rho GTPases by p120-catenin. Curr Opin Cell Biol 2001; 13: 604–610. [PubMed: 11544030]
22. Yanagisawa M, Huveldt D, Kreinest P, Lohse CM, Cheville JC, Parker AS et al. A p120 catenin isoform switch affects Rho activity, induces tumor cell invasion, and predicts metastatic disease. J Biol Chem 2008; 283: 18344–18354. [PubMed: 18407999]
23. Zhang J, Lin Y, Zhang Y, Lan Y, Lin C, Moon AM et al. Frs2alpha-deficiency in cardiac progenitors disrupts a subset of FGF signals required for outflow tract morphogenesis. Development 2008; 135: 3611–3622. [PubMed: 18832393]
24. Ellwood-Yen K, Graeber TG, Wongvipat J, Iruela-Arispe ML, Zhang J, Matusik R et al. Myc-driven murine prostate cancer shares molecular features with human prostate tumors. Cancer Cell 2003; 4: 223–238. [PubMed: 14522256]
25. Israely I, Costa RM, Xie CW, Silva AJ, Kosik KS, Liu X. Deletion of the neuron-specific protein delta-catenin leads to severe cognitive and synaptic dysfunction. Curr Biol 2004; 14: 1657–1663. [PubMed: 15380068]
26. Kosik KS, Donahue CP, Israely I, Liu X, Ochiishi T. Delta-catenin at the synaptic-adherens junction. Trends Cell Biol 2005; 15: 172–178. [PubMed: 15752981]
27. McCrea PD, Park J-I. Developmental functions of the P120-catenin sub-family. Biochim Biophys Acta 2007; 1773: 17–33. [PubMed: 16942809]
28. Paffenholz R, Franke WW. Identification and localization of a neurally expressed member of the plakoglobin/armadillo multigene family. Differentiation 1997; 61: 293–304. [PubMed: 9342840]
29. Kim H, He Y, Yang I, Zeng Y, Kim Y, Seo Y-W et al. δ-Catenin promotes E-cadherin processing and activates β-catenin-mediated signaling: implications on human prostate cancer progression. Biochim Biophys Acta 2012; 1822: 509–521. [PubMed: 22261283]
30. Patiar S, Harris AL. Role of hypoxia-inducible factor-1alpha as a cancer therapy target. Endocr Relat Cancer 2006; 13 Suppl 1: S61–75. [PubMed: 17259560]
31. Poon E, Harris AL, Ashcroft M. Targeting the hypoxia-inducible factor (HIF) pathway in cancer. Expert Rev Mol Med 2009; 11: e26. [PubMed: 19709449]
32. Powis G, Kirkpatrick L. Hypoxia inducible factor-1alpha as a cancer drug target. Mol Cancer Ther 2004; 3: 647–654. [PubMed: 15141023]
33. Bensinger SJ, Christofk HR. New aspects of the Warburg effect in cancer cell biology. Semin Cell Dev Biol 2012; 23: 352–361. [PubMed: 22406683]
34. Dang CV, Kim J, Gao P, Yustein J. The interplay between MYC and HIF in cancer. Nat Rev Cancer 2008; 8: 51–56. [PubMed: 18046334]
35. Podar K, Anderson KC. A therapeutic role for targeting c-Myc/Hif-1-dependent signaling pathways. Cell Cycle 2010; 9: 1722–1728. [PubMed: 20404562]
36. Iwata T, Schultz D, Hicks J, Hubbard GK, Mutton LN, Lotan TL et al. MYC overexpression induces prostatic intraepithelial neoplasia and loss of Nkx3.1 in mouse luminal epithelial cells. PLoS ONE 2010; 5: e9427. [PubMed: 20195545]
37. Kim H, Han J-R, Park J, Oh M, James SE, Chang S et al. Delta-catenin-induced dendritic morphogenesis. An essential role of p190RhoGEF interaction through Akt1-mediated phosphorylation. J Biol Chem 2008; 283: 977–987. [PubMed: 17993462]
38. Kim H, Oh M, Lu Q, Kim K. E-Cadherin negatively modulates delta-catenin-induced morphological changes and RhoA activity reduction by competing with p190RhoGEF for delta-catenin. Biochem Biophys Res Commun 2008; 377: 636–641. [PubMed: 18930028]
39. Dohn MR, Brown MV, Reynolds AB. An essential role for p120-catenin in Src- and Rac1-mediated anchorage-independent cell growth. J Cell Biol 2009; 184: 437–450. [PubMed: 19188496]
40. Liu Y, Li Q-C, Miao Y, Xu H-T, Dai S-D, Wei Q et al. Ablation of p120-catenin enhances invasion and metastasis of human lung cancer cells. Cancer Sci 2009; 100: 441–448. [PubMed: 19154401]
41. Lu Q, Aguilar BJ, Li M, Jiang Y, Chen Y-H. Genetic alterations of δ-catenin/NPRAP/Neurojungin (CTNND2): functional implications in complex human diseases. Hum Genet 2016; 135: 1107–1116. [PubMed: 27380241]
42. DeBusk LM, Boelte K, Min Y, Lin PC. Heterozygous deficiency of delta-catenin impairs pathological angiogenesis. J Exp Med 2010; 207: 77–84. [PubMed: 20048286]

43. Huang F, Chen J, Wang Z, Lan R, Fu L, Zhang L. δ-Catenin promotes tumorigenesis and metastasis of lung adenocarcinoma. Oncol Rep 2018; 39: 809–817. [PubMed: 29251319]
44. Viswanathan SR, Nogueira MF, Buss CG, Krill-Burger JM, Wawer MJ, Malolepsza E et al. Genome-scale analysis identifies paralog lethality as a vulnerability of chromosome 1p loss in cancer. Nat Genet 2018; 50: 937–943. [PubMed: 29955178]
45. Wu Y-M, Cieślik M, Lonigro RJ, Vats P, Reimers MA, Cao X et al. Inactivation of CDK12 Delineates a Distinct Immunogenic Class of Advanced Prostate Cancer. Cell 2018; 173: 1770–1782.e14. [PubMed: 29906450]
46. Ip CKM, Ng PKS, Jeong KJ, Shao SH, Ju Z, Leonard PG et al. Neomorphic PDGFRA extracellular domain driver mutations are resistant to PDGFRA targeted therapies. Nat Commun 2018; 9: 4583. [PubMed: 30389923]
47. Bailey MH, Tokheim C, Porta-Pardo E, Sengupta S, Bertrand D, Weerasinghe A et al. Comprehensive Characterization of Cancer Driver Genes and Mutations. Cell 2018; 173: 371–385.e18. [PubMed: 29625053]
48. Zhang G, Neubert TA. Use of detergents to increase selectivity of immunoprecipitation of tyrosine phosphorylated peptides prior to identification by MALDI quadrupole-TOF MS. Proteomics 2006; 6: 571–578. [PubMed: 16342243]
49. Maere S, Heymans K, Kuiper M. BiNGO: a Cytoscape plugin to assess overrepresentation of gene ontology categories in biological networks. Bioinformatics 2005; 21: 3448–3449. [PubMed: 15972284]
50. Jones SB, Lu HY, Lu Q. Abl tyrosine kinase promotes dendrogenesis by inducing actin cytoskeletal rearrangements in cooperation with Rho family small GTPases in hippocampal neurons. J Neurosci 2004; 24: 8510–8521. [PubMed: 15456825]
51. Jones SB, Lanford GW, Chen Y-H, Morabito M, Kim K, Lu Q. Glutamate-induced delta-catenin redistribution and dissociation from postsynaptic receptor complexes. Neuroscience 2002; 115: 1009–1021. [PubMed: 12453475]

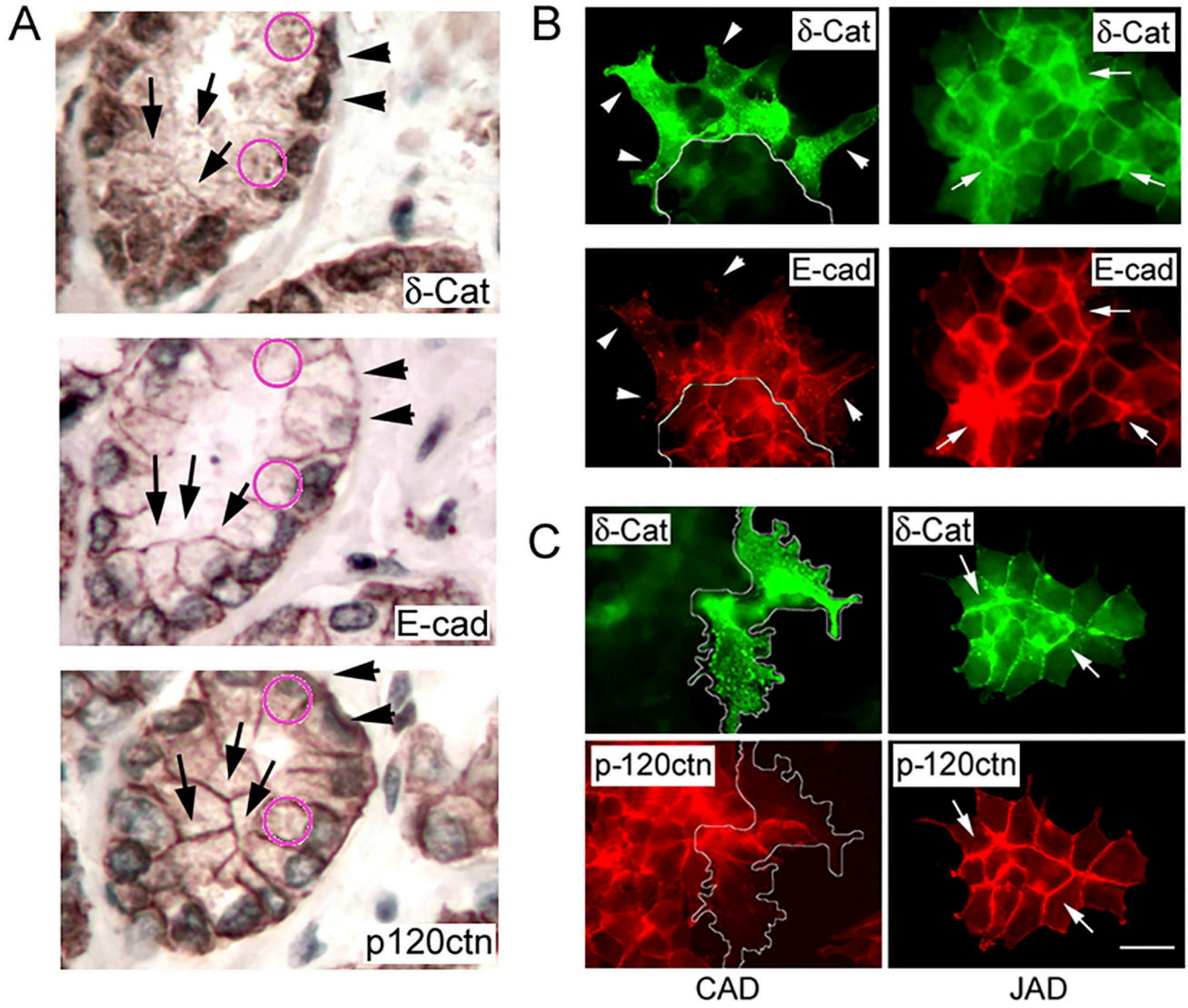

Figure 1: Differential δ-catenin distribution patterns in the same prostate tumor mass and prostate cancer (PCa) xenograft cell line.

A. δ-Catenin, E-cadherin, and p120^{ctn} distribute to cell-cell junctions (arrows) in the luminal side of prostatic tumors. When δ-catenin shows perinuclear (arrowheads) or cytoplasmic (circles) localization towards the tumor periphery, there is weakened E-cadherin (arrowheads) and p120^{ctn} (arrowheads) expression as well as disrupted cell-cell junctions. Under such condition, cytoplasmic δ-catenin (circles) does not colocalize with E-cadherin and p120^{ctn} (circles).

B and C. In PCa xenograft cell line Rv1-M6 that overexpresses δ-catenin (green), δ-catenin also showed differential distribution patterns that mimicked the *in vivo* distribution. B. In the left panels, δ-catenin shows actin-associated AAD or cytoplasmic CAD distribution like bark distribution at the edge of the cell cluster (arrowheads) where E-cadherin (red) expression was diminished (arrowheads). Cells that do not overexpress δ-catenin (green, drawing line) showed clear E-cadherin JAD (red, drawing line). In the right panels, δ-catenin (green) also showed cell-cell junction (arrows) associated JAD distribution where E-cadherin

(red) expression was strong (arrows). C. Similarly, In the left panels, cells that overexpress δ-catenin AAD or CAD (green, drawing line) showed diminished $p120^{ctn}$ co-localization (red, drawing line). In the right panels, δ-catenin (green) showed junction associated JAD distribution (arrows) where $p120^{ctn}$ (red) expression was strong (arrows). Bar: 20 μm.

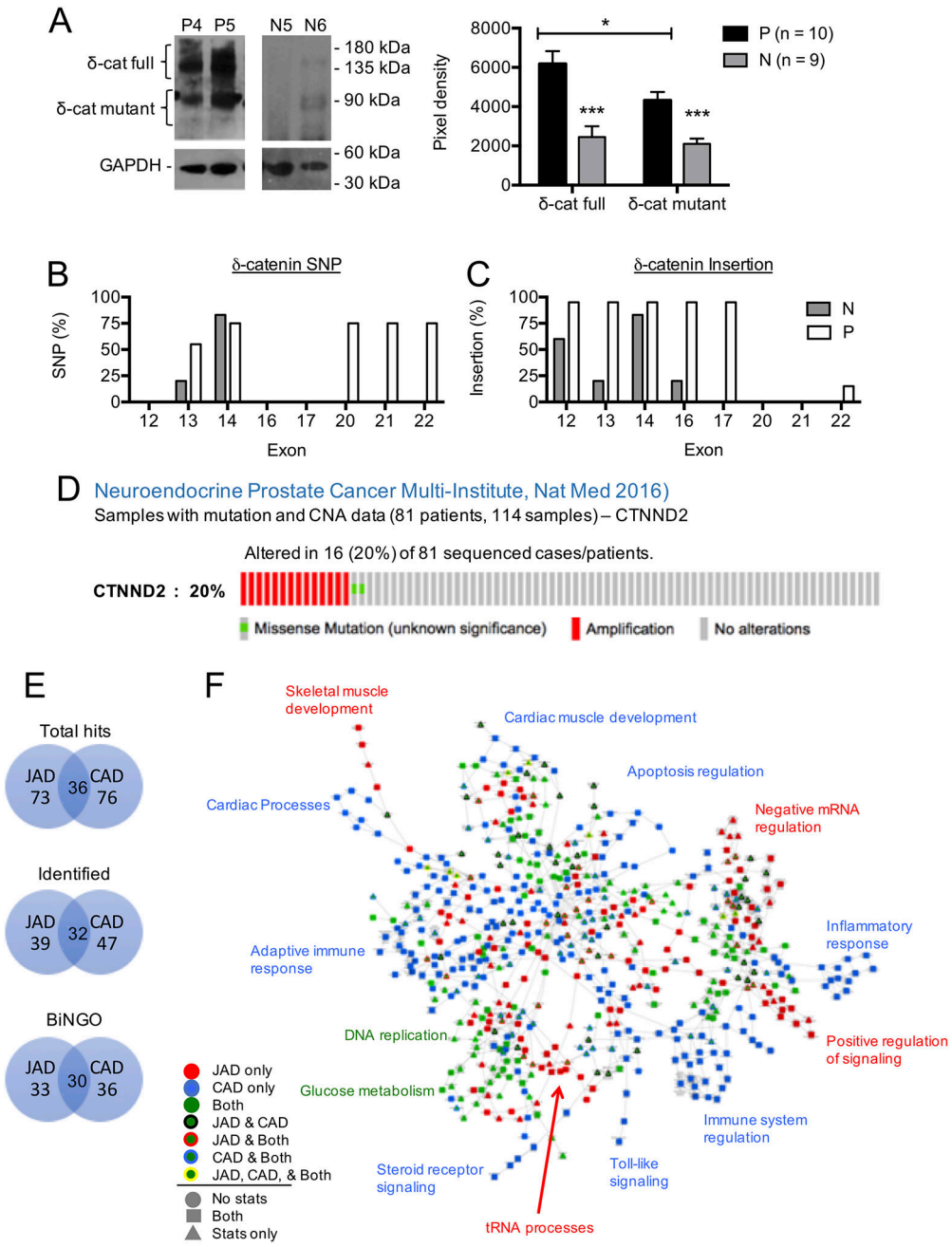

Figure 2: δ-Catenin genetic alterations and non-overlapping interactomes involving distinct biological processes elicited by wildtype and mutant forms of δ-catenin in human PCa.

A. Western blot showing full-length and truncated mutant δ-catenin from lymph node metastasis and control lymph nodes. GAPDH was used as loading controls. P: PCa; N: Normal control.

B. Comparison of mutation rates between PCa patient lymph nodes and normal control.

C. Comparison of rate of gene insertions and fusions between PCa patient lymph nodes and normal control.

D. Frequency of gene alterations in neuroendocrine PCa samples.

E. Overlapping and non-overlapping hits (Venn diagram) generated by δ-catenin JAD and CAD cells.

F. Signaling and biological processes elicited by δ-catenin JAD and CAD cells. Significantly enriched biological processes of proteins present in JAD and/or CAD cells. Statistical analysis was performed with a hypergeometrical test. All processes are statistically modified (increased or decreased) ($p<0.05$).

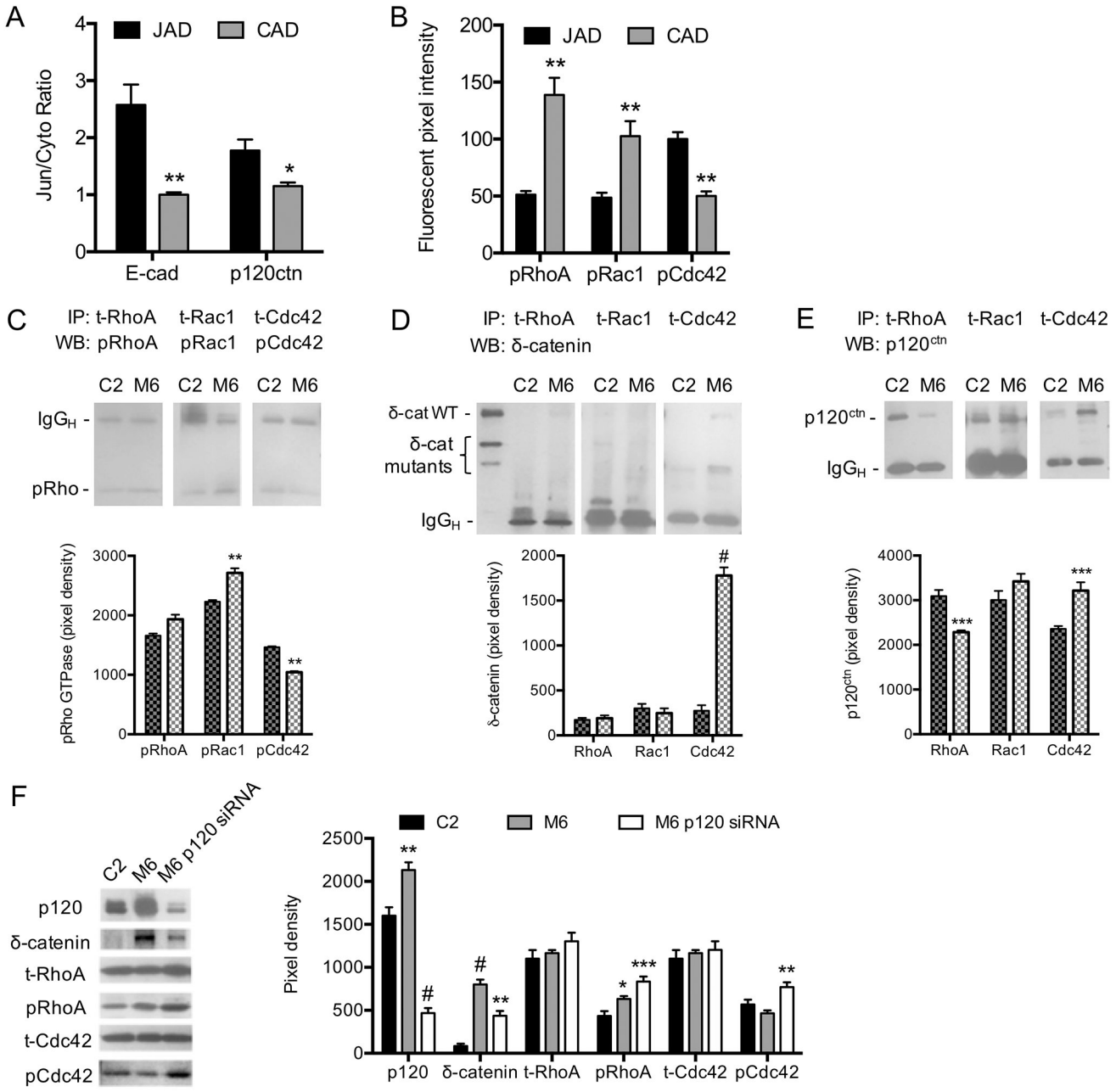

Figure 3: Differential δ-catenin subcellular distribution corresponds to the different fate of E-cadherin/p120^{ctn} and influences the interactions of p120ctn with RhoA, Cdc42, and Rac1.

A. Junction/cytoplasm ratio of E-cadherin and p120^{ctn} in JAD and CAD Rv1-M6 cells.

B. Pixel intensity of phospho-RhoA, Rac1, and Cdc42 in JAD and CAD Rv1-M6 cells.

C. Co-immunoprecipitation of total Rho GTPase and western blot showing phospho-Rho GTPase in CWR22Rv1 cells without (C2) or with (M6) δ-catenin overexpression. Overexpression of δ-catenin increased phospho-Rac1 and decreased phospho-Cdc42 levels.

D. Co-immunoprecipitation of total Rho GTPase and western blot showing δ-catenin (WT and mutant/truncated) interactions in C2 or M6 cells. Mutant/truncated δ-catenin shows increased interactions with Cdc42.

E. Co-immunoprecipitation of total Rho GTPase and western blot showing $p120^{ctn}$ interactions in C2 or M6 cells. Overexpression of δ-catenin decreased $p120^{ctn}$ interactions with RhoA and increased interactions with Cdc42.

F. Knockdown of $p120^{ctn}$ reduced δ-catenin expression. Knockdown of $p120^{ctn}$ further increased phospho-RhoA in Rv1-M6 cells. Knockdown of $p120^{ctn}$ appears to reverse the effects of δ-catenin overexpression on phospho-Cdc42 (M6 versus M6 $p120^{ctn}$ siRNA). All data are presented as mean±SEM from triplicates from at least two independent experiments. Student's t-test or ANOVA compared treatments to their respective control (* $p<0.05$, ** $p<0.01$, *** $p<0.001$, # $p<0.0001$).

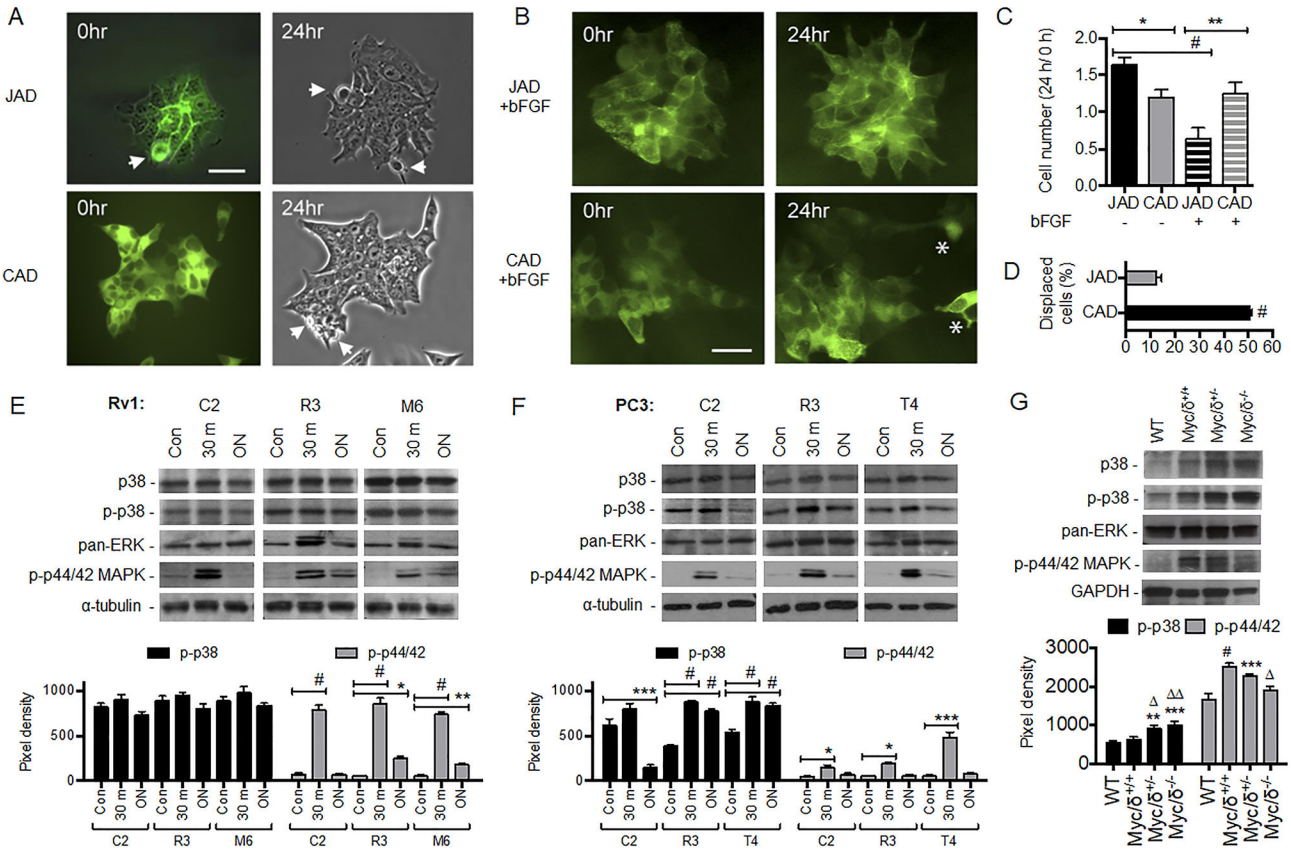

Figure 4: Differential δ-catenin distribution in PCa cells elicits different responses to bFGF stimulation.

A. Time lapse of Rv1-M6 cells. δ-Catenin JAD promoted cell proliferation compared with δ-catenin CAD cells. JAD Rv1-M6 cells showing δ-catenin distribution at cell-cell junction. CAD Rv1-M6 cells showing cytoplasmic δ-catenin distribution. Arrowheads highlight cells in division.

B. δ-Catenin CAD Rv1-M6 cells increased cell proliferation compared with δ-catenin JAD Rv1-M6 cells in response to bFGF treatment. Asterisks highlight cells moving away from the cluster.

C. Quantification of cell proliferation in response to bFGF treatment. Data represent the ratio of cell numbers at 24 hours over that of 0 hour of bFGF treatment. ANOVA comparisons are as indicated (* $p<0.05$, ** $p<0.01$, # $p<0.0001$). Scale bar: 10 μm.

D. Quantification of cell displacement in response to bFGF treatment. Data represent the percentage of cells displaced after time-lapse video recording for 24 hours with bFGF treatment from three independent experimental time-series. For each recording, a minimum of 25 cells were traced for their movement. ANOVA comparisons are as indicated (# $p<0.0001$).

E. Effect of δ-catenin on bFGF induced p38 and p44/42 phosphorylation in transfected Rv1 cells.

F. Effect of δ-catenin on bFGF induced p38 and p44/42 phosphorylation in transfected PC3 cells.

** p <0.01, *** p <0.001, # p <0.0001 compared to Control. All data are presented as mean±SEM from triplicates from at least two independent experiments. Student's t-test or ANOVA compared treatments to their respective control.

G. Effect of δ-catenin on p38 and p44/42 phosphorylation in Myc/δ-catenin mutant mice. ** p <0.01, *** p <0.001, # p <0.0001 compared to WT. Δ p <0.05, ΔΔ p <0.01 compared to Myc/$\delta^{+/+}$. All data are presented as mean±SEM from triplicates from at least two independent experiments. Student's t-test or ANOVA compared treatments to their respective control.

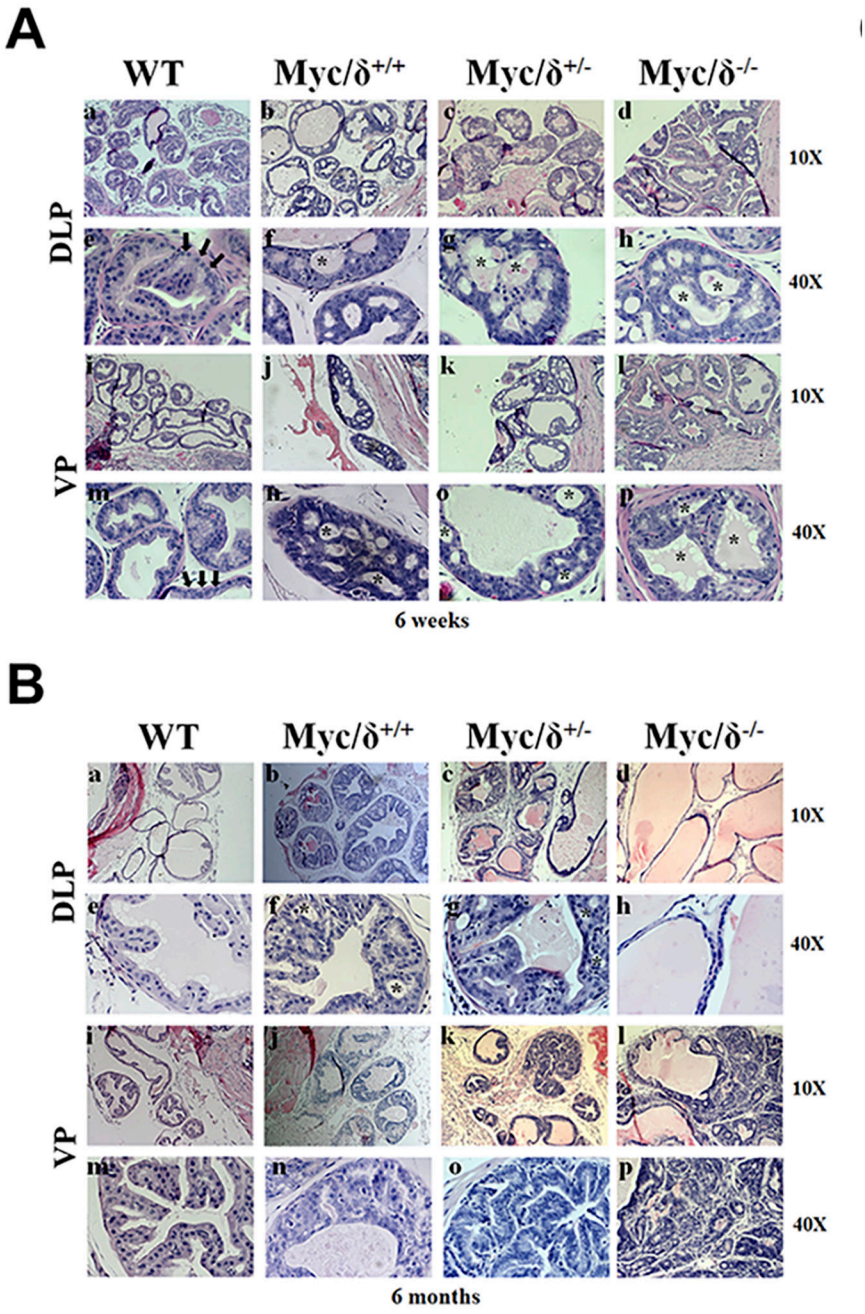

Figure 5: δ-Catenin promotes prostate tumor development in a mutation dependent manner.

A. Histopathology analysis (H&E) of wild type (WT), Myc/$\delta^{+/+}$, Myc/$\delta^{+/-}$, and Myc/$\delta^{-/-}$ mice. Prior to tumor onset (6-week-old-mice). Arrows point to the glandular epithelia. mPIN lesions, recognized by intraepithelial space formation (indicated by asterisks), are found in transgenic animals (f-h and n-p) regardless of prostate regions.

B. Histopathology (H&E) of 6 month-old-mice from WT, Myc/$\delta^{+/+}$, Myc/$\delta^{+/-}$, and Myc/$\delta^{-/-}$. Note that only Myc/$\delta^{-/-}$ mice showed diffuse, invasive prostate adenocarcinoma with large, undifferentiated tumor cells growing into stromal areas (l and p) in VP, while

DLP (b-c and f-g) and VP (j-k and n-o) of Myc/$\delta^{+/+}$ and Myc/$\delta^{+/-}$prostates continued to exhibit mPIN lesions at the same time point.

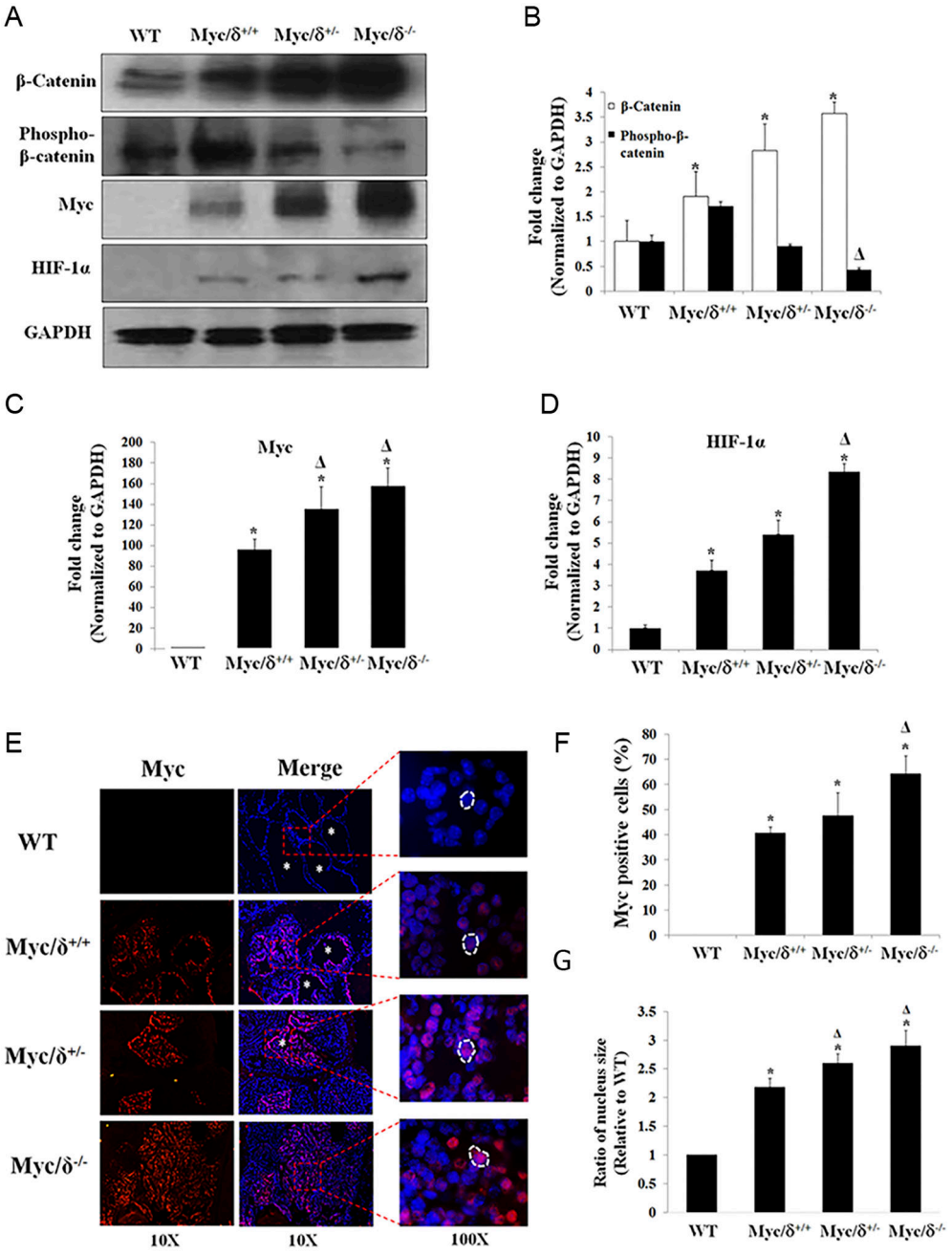

Figure 6: δ-Catenin mutations enhance β-catenin, Myc, and HIF-1α expression.

A. Representative Western blot analysis of six month-old mouse prostate lysate probed with antibodies against β-catenin, phosphorylated β-catenin, Myc, and HIF-1α. GAPDH served as a loading control.

B - D. Graphs represent quantitative measurement of Western blot band intensities with the indicated proteins. It was shown that δ-catenin mutations resulted in significant increased β-catenin and Myc expressions, but decreased phosphorylated-β-catenin, which was associated with doses of δ-catenin mutations. These results suggested the reduction of β-catenin degradation. Results shown are mean±SEM from two independent experiments. All data

was normalized to loading control and represented in fold induction versus wild type (* $p< 0.01$) or Myc/$\delta^{+/+}$ (Δ $p<0.01$).

E. Anti-Myc (red) and Hoechst (nuclei marker, blue) immunofluorescent analysis of 5 μm mouse ventral prostate cross sections at 6 months of age from Myc/δ-cat mutant mice. Results revealed that Myc overexpression in Myc/$\delta^{+/+}$ and Myc/$\delta^{+/-}$ prostates predominantly localized to luminal epithelia as indicated by white asterisks in luminal compartments of prostate glands whereas Myc overexpression in Myc/$\delta^{-/-}$ prostates showed widespread distribution beyond the lumen (left and middle panels). Note that an age matched wild-type (WT) prostate was completely negative staining for Myc. The 100x enlargement showed increased nuclear size in cells with Myc expression in Myc/$\delta^{-/-}$ prostates.

F. Number of cells overexpressing Myc increases dramatically, notably when prostate basement membranes were no longer intact as shown in Myc/$\delta^{-/-}$ (right panel). Values represent mean±SEM for a total of 500 cells counted from two sets of independent experiments.

G. The nuclear area was randomly measured and calculated in total of 100 cells. Results were reported as a fold induction from WT. * $p<0.01$, relative to WT and Δ $p<0.05$, relative to Myc/$\delta^{+/+}$.

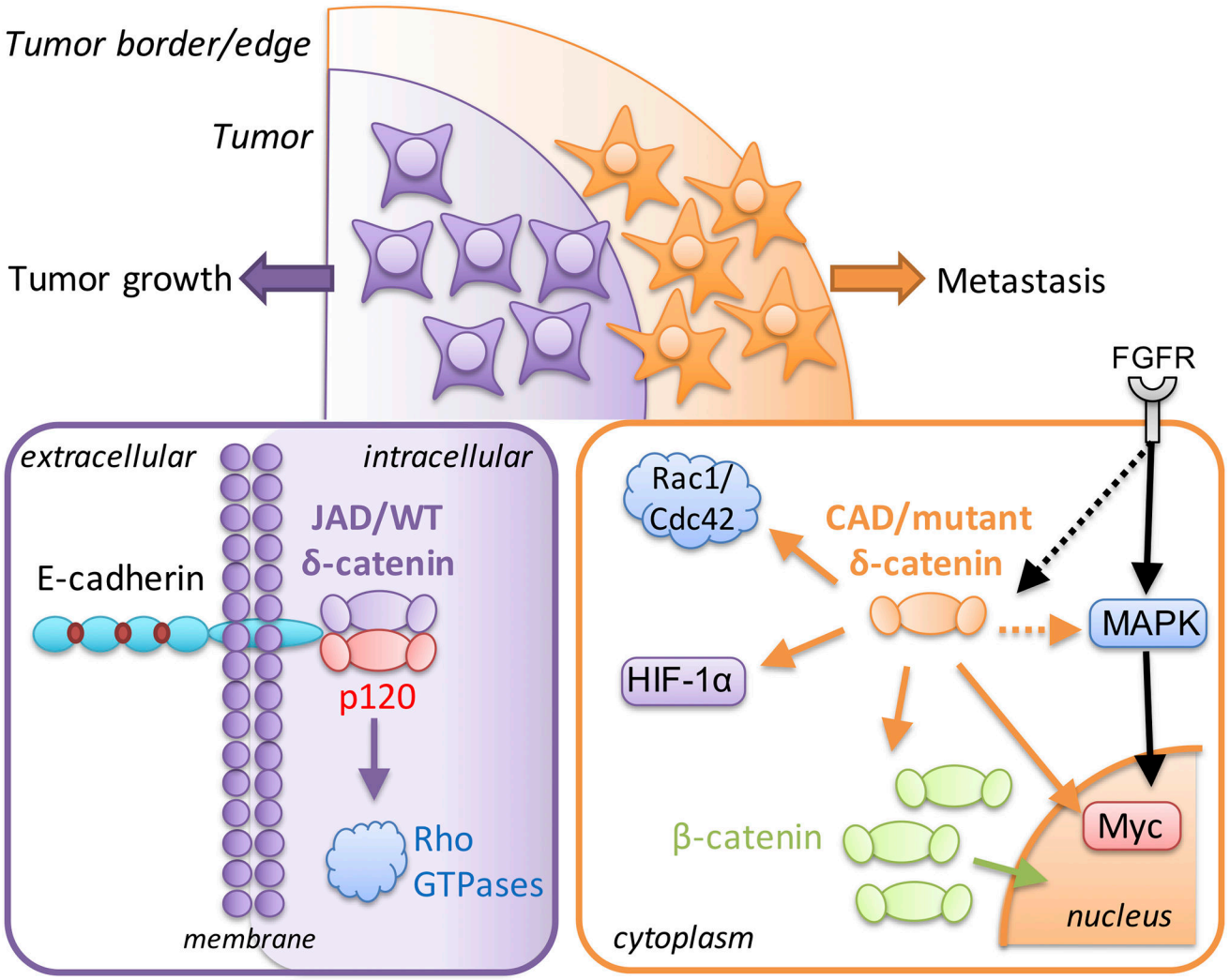

Figure 7: Schematic showing the model of intratumor heterogeneity of δ-catenin in modulation of PCa cell dissemination.

Prostatic tumors may harbor subpopulations of JAD/WT and CAD/mutant δ-catenin cells. Inside the tumor (purple), JAD/WT δ-catenin is colocalized with E-cadherin and $p120^{ctn}$ and regulates Rho GTPases to affect its cancer signaling. At the tumor border/edge (orange), CAD/mutant δ-catenin is found in the cytoplasm, which increases Myc-dependent tumor progression rate, activates Rac1/Cdc42, and increases β-catenin levels resulting in increased translocation to the nucleus to facilitate tumorigenesis. CAD/mutant δ-catenin may reprogram MAPK from p44/42 to p38 in response to bFGF stimulation leading to increased cell motility and metastasis.